JETIR.ORG ISSN: 2349-5162 | ESTD Year : 2014 | Monthly Issue
JOURNAL OF EMERGING TECHNOLOGIES AND INNOVATIVE RESEARCH (JETIR)
An International Scholarly Open Access, Peer-reviewed, Refereed Journal

ABID (Automated Bleeding Image Detection) Using fully convolutional network (FCN) and Combined Texture and Color Features.

Mrs R Anitha , Mrs N Juliet, Mrs K Malathy, Mrs R Rajeshwari
[1] Research scholar/Assistant Professor,SA Engineering College, Chennai-77
2 Associate professor,SA Engineering College, Chennai-77.
3 Assistant professor,SA Engineering College, Chennai-77.
4 Assistant professor,SA Engineering College, Chennai-77.

Abstract : Wireless capsule endoscopy (WCE) is a technique that is increasingly being utilized to visualize the gastrointestinal (GI) tract. Capsule endoscopy exams are typically suggested as an additional monitoring mechanism and can aid in the detection of polyps, bleeding, and other abnormalities. Automatic image processing, computer vision, and learning algorithms are required to assess the vast volume of video data generated by WCE examinations. Recently, methods for automatic polyp detection have been presented, with varying degrees of effectiveness. While bleeding detection in colonoscopy and other standard endoscopic procedure-based images is maturing, detecting bleeding automatically in WCE is a difficult problem due to its unique imaging properties. This article takes a deep neural network method and offers a model called ABID (Automated Bleeding Image Detection) for classifying WCE bleedy images. It combines a color feature extraction layer with a fully convolutional network (FCN) model. ABID initially computes using the FCN model due to its reduced computational power demand, and then feeds the output to the CNN for further processing. A dataset of 1550 WCE images is used to train and test the model. The performance of the ABID is evaluated using the accuracy, precision, recall, and F1 score. The results reveal that the accuracy, precision, recall, and F1 score obtained were 94.51, 98.3, 94, and 97, respectively.

IndexTerms **-. Wireless Capsule Endoscopy, Image Segmentation, Image Pre-Processing, CNN, Polyp Detection, Deep Learning.**

I. INTRODUCTION

The human digestive system is incomplete without the small intestine. It is located between the large and small intestines [10][11]. Most disorders of the human stomach, such as tumors, inflammation, and hemorrhage, can be easily managed and treated if detected early. However, early detection of many disorders is quite challenging. Gabi Iddan and Paul Swain created the WCE in 1997. The research of the gastrointestinal system has been simplified by the advancement of technology. Through a painless method, wireless capsule endoscopy (WCE) enables clinicians to check the inner wall of the human gastrointestinal tract. Because this treatment has no adverse effect on the patients during the diagnostic process, it has gained widespread acceptance among doctors and patients. For diagnostic purposes, the accuracy of WCE images is crucial.

The traditional WCE system incorporates a pill-shaped electronic capsule, an RF data recorder, and a programmable desktop computer computer [12][13][14]. The capsule is equipped with a light source, an image sensor, a contact module, and batteries. After the patient swallows the capsule, it begins capturing images and transferring them to the data recorder through the RF transmitter. The data recorder is responsible for receiving and storing data. Using image processing tools, the physician reviews the images. The software flags frames that are suspected of holding anomalies for further investigation by the physician. This is a lengthy and labor-intensive process [13]. Numerous attempts have been made throughout the years to segment bleeding and polyp in WCE images. Nonetheless, it remains a difficult task.

This study applied a deep neural network method to classify WCE bleed images and proposes the model ABID (Automated Bleeding Image Detection). It combines a layer for extracting color features with a model for fully convolutional network (FCN). Due to the MobileNet model's lower computational power requirement, ABID computes initially and then feeds the output to the CNN for additional processing. The model is trained and tested using a dataset of 1550 WCE photos. The accuracy, precision, recall, and F1 score are used to measure the ABID's performance. The accuracy, precision, recall, and F1 score obtained in this study were 94.51, 98.3, 94, and 97, respectively.

We provide an overview of the many automatic image/video data-based polyp and bleeding identification (localization) and segmentation approaches proposed in the literature. Then discuss the remaining difficulties of existing polyp and bleeding detection systems. The remainder of the paper is organized as follows: Section 2 reviews the literature on polyp and bleeding detection, segmentation, and holistic approaches. In Section 3, we explore the future of this discipline and the obstacles that must be overcome through future research.

II. Literature Review

The purpose of this section is to summarize the research on bleeding detection in wireless-capsule endoscopic images, with an emphasis on machine learning, deep learning and other image processing algorithms and methods. Significant research in this arena enables automatic disease screening from a wide number of visual data, which saves medical experts both time and effort and improves diagnosis efficiency. Automatic identification of viral photos has been a hot topic of research in recent years, with a plethora of material available in the literature. In essence, these research employ three types of techniques: classical machine learning algorithms such as SVM, k-NN, and others, proposed/modified models such as modified PCA, and deep learning techniques such as convolutional neural networks (CNN), multilayered perceptron, and others.

The study [1] classified bleedy and normal images using a support vector machine (SVM) using a radial basis function and achieved an accuracy of 0.978. The study [2] classified bleedy and non-bleedy frames using the Contourlet transform and a local binary pattern (LBP). They attain a 0.963 percent accuracy using the k-Nearest Neighbor (k-NN) classifier. The study [3] developed an algorithm that eliminates the need for iterations, approximations, and inversion operations by combining a joint diagonalization principal component analysis (PCA) with the color coherence vector (CCV). This technique resolves the PCA issue and the 'curse of dimensionality' associated with the original asymptotic PCA.

The study [1] provided a method for automatically detecting gastrointestinal tract infection in the presence of numerous diseases and abnormalities. The study employs a color features and texture features-based technique for detecting bleeding. The color information in the image is used to extract the lesion. While color information is critical for the initial detection of bleeding images, texture information can be used to remove lesions from the identified images. The proposed technique is capable of making precise distinctions between borderline cases. Another work [4] suggested an approach for segmenting bleedy WCE frames by extracting texture features from the HIS intensity channel and classifying the frames using support vector machines. They calculated the mean, variance, entropy, kurtosis, skewness, and energy of the uniform LBP with eight areas. The study [5] suggested a method for classifying abnormalities such as bleeding and ulcers by combining an ANOVA with the F-statistics measure and a sequential floating forward search to categorize frames based on color and texture attributes.

Recently, various deep learning algorithms for the automatic detection of infection lesions using WCE pictures have been proposed and implemented. For instance, the study [6] detected the bleedy zone in WCE video using chrominance-moment-based texture. To distinguish normal and bleeding regions in WCE pictures, this study used a multilayered perceptron neural network. Similarly, [7] employed deep convolutional neural networks to detect Ulcer using WCE photos. They presented the HAnet architecture, which is based on ResNet-34. During the WCE procedure, a dataset of 1,416 separate movies is collected, and frames from these videos are later used in the study.

HAnet's accuracy score is 92.05 percent, while its sensitivity and specificity are 91.64 and 92.42 percent, respectively. In a similar vein, the author uses a CNN model to diagnose middle ear disorders in [8]. They diagnose the tympanic membrane using the CNN model. A six-layer CNN is constructed, and features are extracted using a class activation map. CNN performs admirably, achieving 97.9 percent accuracy. These studies demonstrate the potential for deep learning approaches to be used in medical imaging categorization.

III. Proposed Method

The suggested system is a feature extraction technique that makes use of texture and color. Fig.1 illustrates the overall graphical representation of the proposed ABID (Automated Bleeding Image Detection).

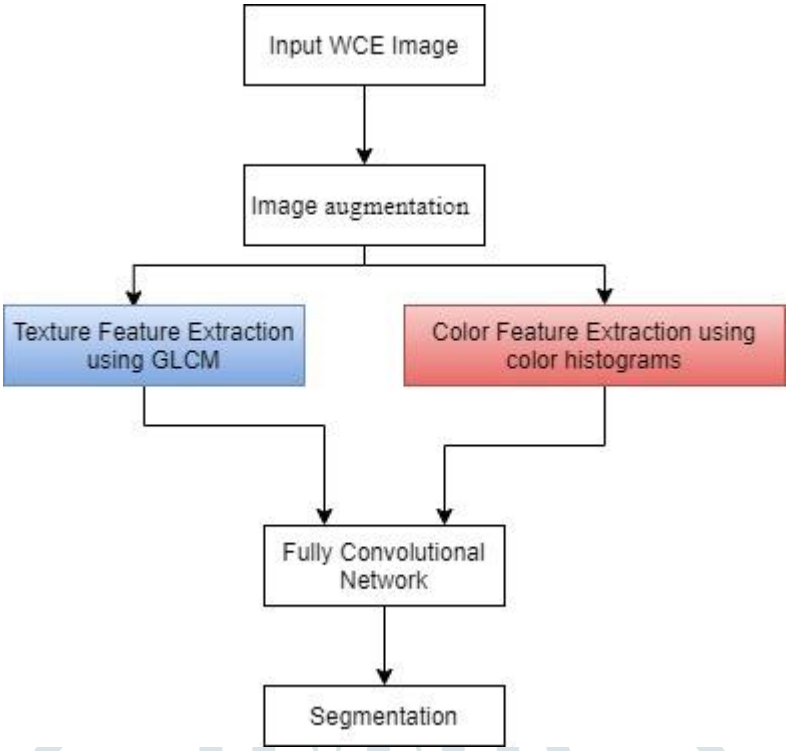

Figure1 Overall architecture of the proposed Automated Bleeding Image Detection

A. Image augmentation

Only when there is sufficient training data can the convolutional neural network work more effectively. Enhancement of images is critical for achieving a better outcome with a little training data set. The use of image augmentation simplifies the training procedure and increases classifier accuracy. Virtual image augmentation is accomplished using a range of computer vision techniques, includes flipping, shifters, and randomized rotation. In this study, the WCE image is enhanced by rotating it 90,180,270 degrees and flipped it.

B. Color Feature Extraction

Color is another essential feature extraction technique for bleeding classification. If a specific location is impacted, the WCE image region effectively changes color. To identify the bleeding, relative color histograms in several color spaces are generated. The three-dimensional histogram is created in color spaces such as RGB, LAB, HSV, HUE, and OPP [12]. The RGB color space is composed of the primary colors Red, Green, and Blue. The color component is represented by these three colors' mixture coefficients. The disadvantages of color spaces are that they are not perceptually homogeneous, and they vary depending on the acquisition configuration. It establishes a high degree of association between these three colour channels. To address these shortcomings, various color representation have already been suggested. For example, edges are enhanced in biologically inspired color spaces such as the opponent color space (OPP), hue saturation and brightness (HSV and HIS), which are color spaces similar to how humans describe color, and CIE La*b* and L*uv, which are perceptually uniform color spaces. This feature vector is fed into the FCN classifier in order to determine the sensitivity and specificity.

C. Texture Feature Extraction

In empirical texture classification, texture characteristics at specified positions relative to one another in an image are extracted from the distribution of intensities. Texture statistics are categorized as first order, second order, and higher order. The Gray Level Co-occurrence Matrix is used to extract second order statistical texture properties (GLCM). The first order texture measure is independent of the pixel neighbor relationships and is calculated directly from the source image. GLCM takes into account the relationship between two pixels, referred to as the reference pixel and a neighbor pixel. A GLCM is a matrix with the same number of rows and columns as the grey levels G in an image. P I j | x, y) is the relative frequency matrix element, where I and j indicate the intensity and are separated by a pixel distance x, y. The GLCM matrix can be used to compute many textural properties such as energy, entropy, contrast, homogeneity, correlation, dissimilarity, inverse difference moment, and maximum probability.

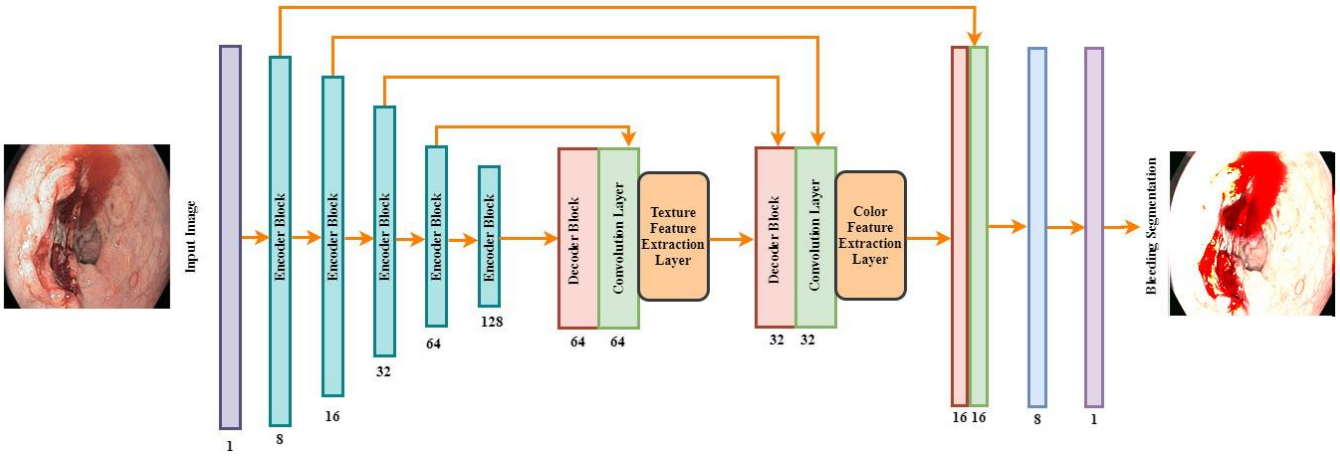

Figure 2 proposed FCN architecture for bleeding region segmentation.

D. Bleeding classification using FCN

Three primary types of layers are used to construct FCN architectures: convolutional layers, subsampling or pooling layers, and totally connected layers. The first layer is a convolutional layer of size [W H D], where W specifies the width of the input image, H signifies the height of the input image, and D denotes the dimension of the input picture. W and H are typically equivalent in image classification applications, while D denotes the number of channels in the input image. Each layer has K filters of size [F F Q], where F should be smaller than W; these filters may be as little as 2×2 or as large as 5×5, with Q being the number of channels in the input image in the first convolutional layer. The second layer is a sub-sampling layer whose primary goal is to gradually reduce the representation's spatial scale. As a result, this technique aids in preventing over fitting by minimizing the amount of parameters and computations required by the network. The final layer is a fully connected layer. In this layer, neurons are connected to all activation units from the preceding layer, and their activations are calculated using matrix multiplication. The first five layers consist of a convolutional layer with 2,4,8,16, and 32 feature maps, each with a kernel size of 33 pixels, and a ReLU activation function that accepts images with 32×32 pixel values. This layer represents our FCN input layer. Following that, we'll discuss two fully connected layers that make use of the maximum value; this layer has a pool size of two. Following that is an up sampling layer. To avoid over fitting, it is programmed to remove 0.2 neurons at random. Our suggested CNN approach is illustrated in Figure 2.

IV. RESULTS AND DISCUSSION

A. Hardware Configuration

In this research, the computer configuration used to execute the software is as follows: GPU: NVIDIA GeForce GTX 960; CPU: Intel(R) Core(TM) i5-4660 3.20 GHz. The operating system is Windows 10, and the software configuration includes Matlab and image processing packages.

B. Dataset Details

To determine the efficiency of the suggested method, various WCE pictures are obtained from a regularly used publicly available database. The database contains ground truth labelling for pictures with and without bleeding. The simulation results are displayed on 1550 WCE images, 800 of which are bleeding and 750 of which are not. A qualified physician reviews visually on bleeding photographs and, if necessary, trims out bleeding zones.

The suggested FCN-based strategy for bleeding area identification in WCE images is compared with the conventional deep learning-based systems on the basis of the most critical accuracy metrics, namely Total Accuracy (TA), Precession (PRE), Recall (REC), and F1-Measure (F1-M). Each of these performance indicators varies depending on the accuracy criteria listed below.

True Positive WCE images bleeding region segmentation: If the proposed approach correctly segments the bleeding zone from varied color and dark backdrop images of the inner GI tract, it is considered to as true positive WCE images bleed area classification. This is determined by the variable TP.

True Negative WCE images bleeding region segmentation: If the suggested technique successfully segments non-bleeding areas from complex color and darker backdrop WCE images, it is considered to as true negative WCE image bleeding region segmentation. This is determined by the variable TN.

False Positive WCE images bleeding region segmentation: If the suggested method unable to effectively separate bleeding regions due to the complicated color and dark background of the Gastrointestinal system, this is considered to as False Positive WCE image bleeding segmentation. This is determined by the variable FP.

False Positive WCE images bleeding region segmentation: If the proposed technique unable to successfully separate non-bleeding regions from WCE images due to complex color and darkened background, this is referred to as False Negative WCE bleeding region segmentation. This is determined by the variable FN.

The total accuracy (TA) of the proposed FCN prediction models is determined by Equation 1.

$$TA = \frac{TP+TN}{TTP+TN+FP+FN} \quad (1)$$

Equation 2 determines the precession rate (PRE) of the proposed FCN prediction model.

$$PRE = \frac{TP}{TP+FP} \quad (2)$$

The recall rate (REC) of the proposed FCN prediction models is computed using equation 3.

$$REC = \frac{TP}{TP+FN} \quad (3)$$

Equation 4 determines the F1-Measure (F1) of the suggested FCN prediction model.

$$F1 = \frac{2(PRE \times REC)}{\text{PRE+REC}} \quad (4)$$

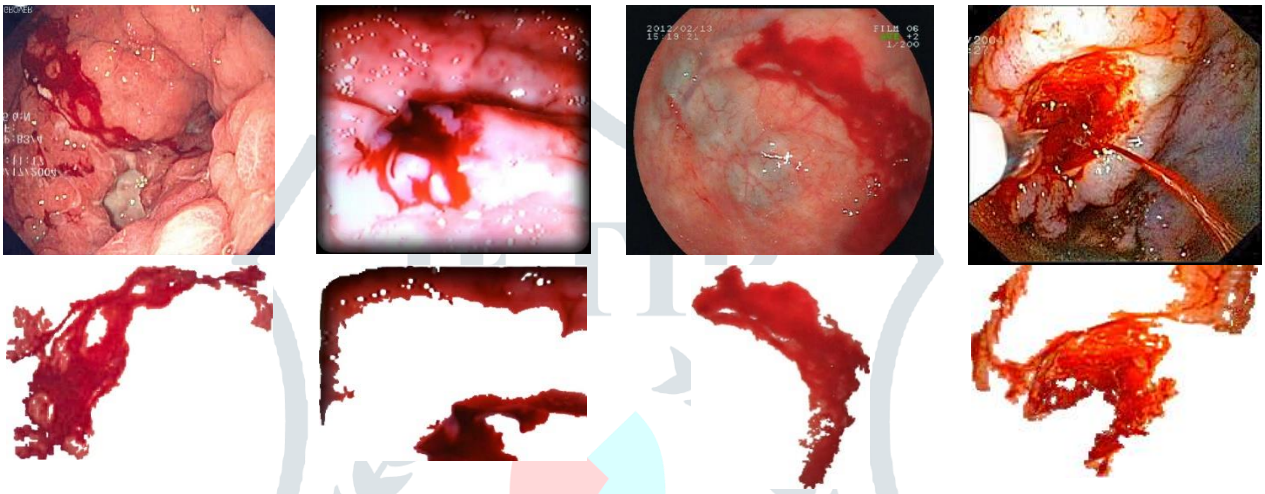

Figure 3 Experimental results

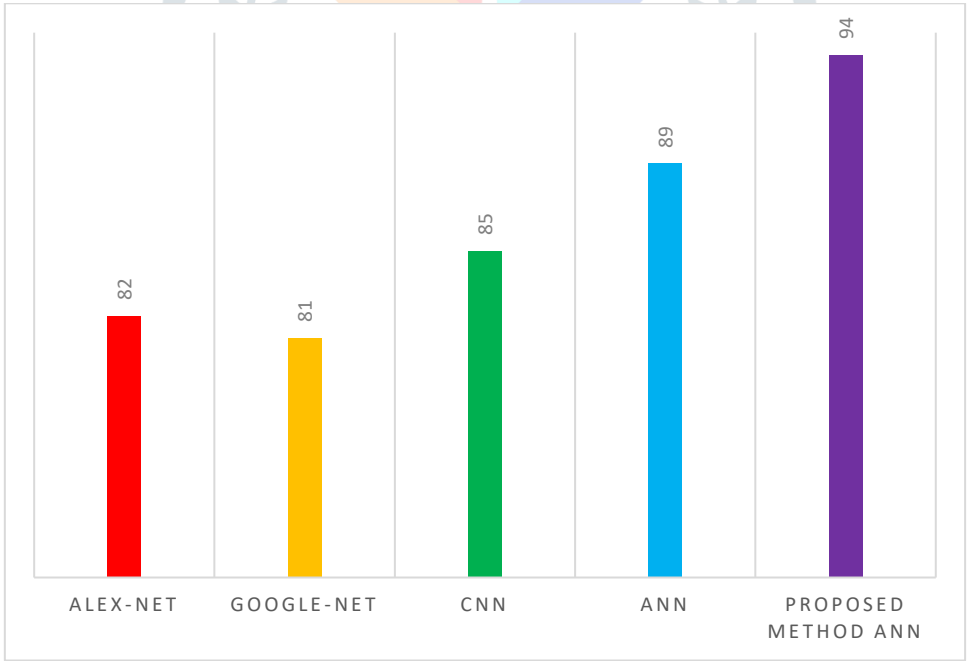

Figure 3. Total accuracy comparison of proposed FCN with existing deep learning based bleeding region segmentation methods.

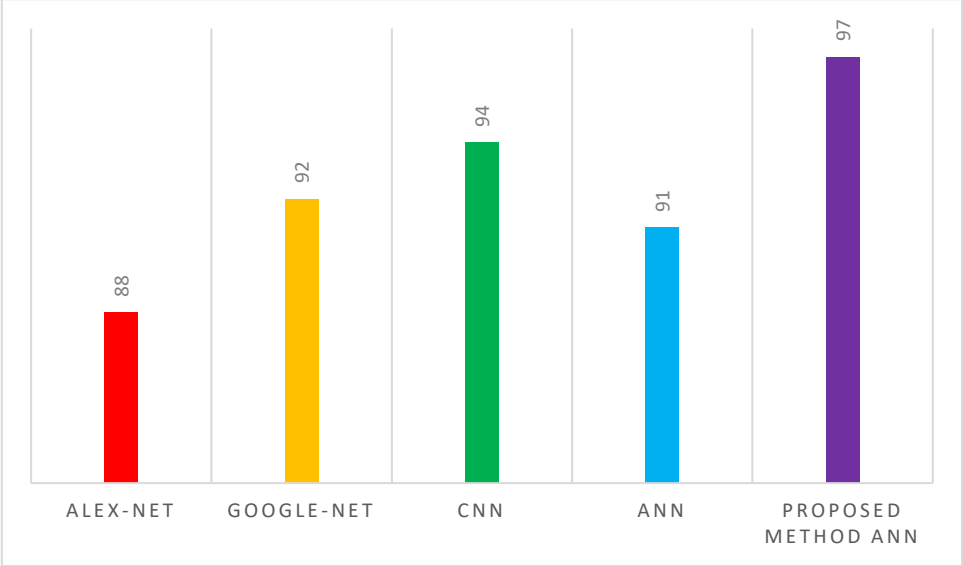

Figure 4. Precession rate comparison of proposed FCN with existing deep learning based bleeding region segmentation methods.

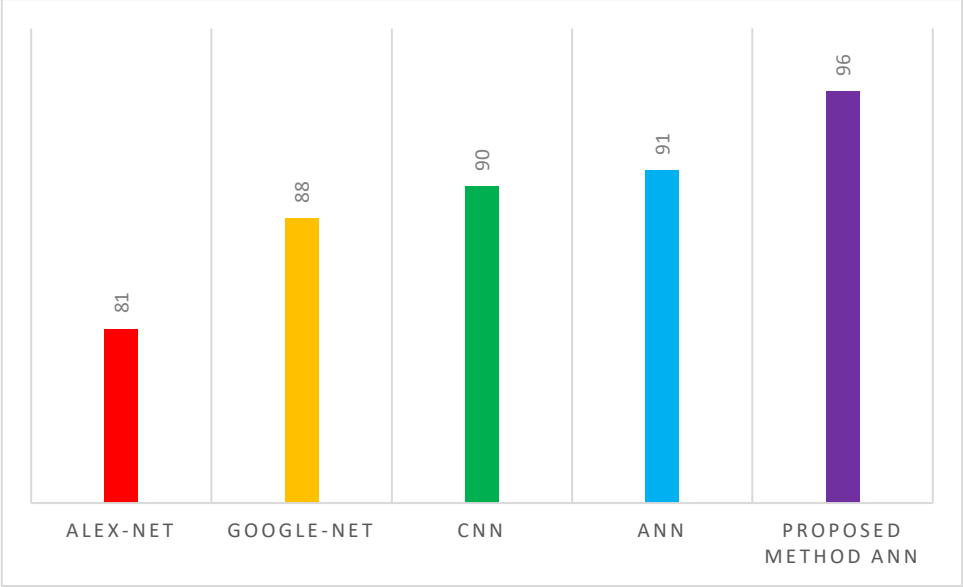

Figure 5. Recall rate comparison of proposed FCN with existing deep learning based bleeding region segmentation methods.

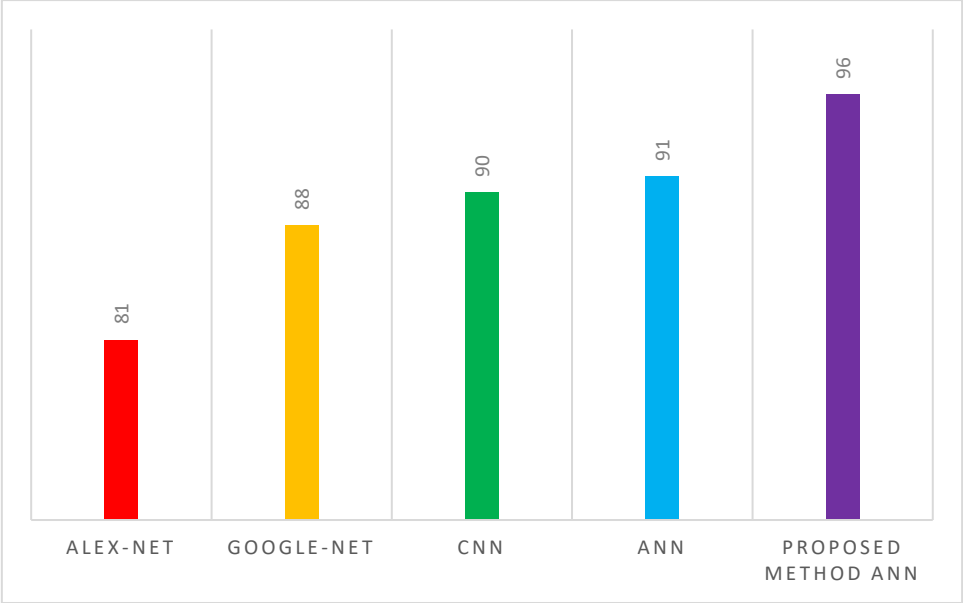

Figure 6. F1-messoure comparison of proposed FCN with existing deep learning based bleeding region segmentation methods.

The new and existing methodologies were experimentally compared to demonstrate the suggested FCN-based approach's forecasting accuracy for WCE bleeding region identification. Visual representation of the comparison results is shown in Figure 4, 5 and 6. The suggested technique collects strongly correlated texture and color features and then feeds them into the FCN model. The proposed approach for segmenting WCE images' bleeding regions achieves the highest accuracy ratio of 94%, 97%, 96% and 96% respectively. This is mostly because the suitable feature extraction method is used. The experimental results indicate that the FP rate of the proposed approach has decreased. As a result, accuracy, recall and precession rate are enhanced.

V. CONCLUSION

Wireless capsule endoscopy is a medical breakthrough. This enables the early diagnosis of a number of gastro-intestinal illnesses. The modified FCN approach is utilized in this proposed research, and therefore bleeding segmentation is accomplished. Combining color and texture features improves the performance of the FCN architecture. As a result, the intricate complexity of network architecture is altered. Additionally, the accuracy and speed with which bleeding segmentation is performed have been significantly enhanced. The experimental results demonstrate this.

REFERENCES

[1] K. Pogorelov, S. Suman, F. A. Hussin, A. S. Malik, O. Ostroukhova, M. Riegler, P. Halvorsen, S. H. Ho, and K. Goh, ‘‘Bleeding detection in wireless capsule endoscopy videos—Color versus texture features,’’ J. Appl. Clin. Med. Phys., vol. 20, no. 8, pp. 141–154, Aug. 2019.

[2] M. Mathew and V. P. Gopi, ‘‘Transform based bleeding detection technique for endoscopic images,’’ in Proc. 2nd Int. Conf. Electron. Commun. Syst. (ICECS), Feb. 2015, pp. 1730–1734.

[3] D.-Y. Liu, T. Gan, N.-N. Rao, Y.-W. Xing, J. Zheng, S. Li, C.-S. Luo, Z.-J. Zhou, and Y.-L. Wan, ‘‘Identification of lesion images from gastrointestinal endoscope based on feature extraction of combinational methods with and without learning process,’’ Med. Image Anal., vol. 32, pp. 281–294, Aug. 2016.

[4] E. Tuba, M. Tuba, and R. Jovanovic, ‘‘An algorithm for automated seg mentation for bleeding detection in endoscopic images,’’ in Proc. Int. Joint Conf. Neural Netw. (IJCNN), May 2017, pp. 4579–4586.

[5] P. Szczypiński, A. Klepaczko, M. Pazurek, and P. Daniel, ‘‘Texture and color based image segmentation and pathology detection in capsule endoscopy videos,’’ Comput. Methods Programs Biomed., vol. 113, no. 1, pp. 396–411, Jan. 2014.

[6] Li and M. Q.-H. Meng, ‘‘Computer-aided detection of bleeding regions for capsule endoscopy images,’’ IEEE Trans. Biomed. Eng., vol. 56, no. 4, pp. 1032–1039, Apr. 2009.

[7] S. Wang, Y. Xing, L. Zhang, H. Gao, and H. Zhang, ‘‘Deep convolutional neural network for ulcer recognition in wireless capsule endoscopy: Experimental feasibility and optimization,’’ Comput. Math. Methods Med., vol. 2019, pp. 1–14, Sep. 2019.

[8] J. Y. Lee, S.-H. Choi, and J. W. Chung, ‘‘Automated classification of the tympanic membrane using a convolutional neural network,’’ Appl. Sci., vol. 9, no. 9, p. 1827, May 2019.

[9] S. S. Chaturvedi, K. Gupta, and P. S. Prasad, ‘‘Skin lesion analyser: An efficient seven-way multi-class skin cancer classification using mobilenet,’’ in Proc. Int. Conf. Adv. Mach. Learn. Technol. Appl. Singapore: Springer, 2020, pp. 165–176.

[10] BORGSTROM B, DAHLQVIST A, LUNDH G, SJOVALL J. Studies of intestinal digestion and absorption in the human. J Clin Invest. 1957;36(10):1521-1536. doi:10.1172/JCI103549.

[11] Fernández-Pérez, S.; Pérez-Andrés, J.; Gutiérrez, S.; Navasa, N.; Martínez-Blanco, H.; Ferrero, M.Á.; Vivas, S.; Vaquero, L.; Iglesias, C.; Casqueiro, J.; Rodríguez-Aparicio, L.B. The Human Digestive Tract Is Capable of Degrading Gluten from Birth. Int. J. Mol. Sci. 2020, 21, 7696. https://doi.org/10.3390/ijms21207696.

[12] Hijaz NM, Attard TM, Colombo JM, Mardis NJ, Friesen CA. Comparison of the use of wireless capsule endoscopy with magnetic resonance enterography in children with inflammatory bowel disease. World J Gastroenterol. 2019;25(28):3808-3822. doi:10.3748/wjg.v25.i28.3808.

[13] Bang CS, Lee JJ, Baik GH. Computer-Aided Diagnosis of Gastrointestinal Ulcer and Hemorrhage Using Wireless Capsule Endoscopy: Systematic Review and Diagnostic Test Accuracy Meta-analysis [published correction appears in J Med Internet Res. 2022 Jan 11;24(1):e36170]. J Med Internet Res. 2021;23(12):e33267. Published 2021 Dec 14. doi:10.2196/33267.

[14] Spada C, McNamara D, Despott EJ, et al. Performance measures for small-bowel endoscopy: A European Society of Gastrointestinal Endoscopy (ESGE) Quality Improvement Initiative. United European Gastroenterol J. 2019;7(5):614-641. doi:10.1177/2050640619850365.